Mathematical modeling of the impact of vehicles on water-saturated soil

Highlights

- A method has been developed to assess the impact of a wheel on waterlogged forest soil.
- The form of the transverse loading diagram has a significant effect on the degree of the stress state of the soil.
- Tires with reduced internal air pressure have the least impact on the ground.
- An application has been developed to assess the degree of soil compaction and the intensity of rutting during the operation of a forest machine.

Abstract

The presented mathematical model, together with its software implementation, makes it possible to assess the degree of influence of a vehicle on waterlogged forest soil, depending on the design parameters of the tire and the vertical loads on it.

The adequacy of the mathematical model is confirmed by the conducted experimental studies, as well as by numerous test results of forest machines.

The model is developed based on the theory of soil mechanics. The plane problem of compaction of water-saturated anisotropic (in the general case) soil is considered. It was shown that with an instantaneous application of a vertical load, the initial distribution of stress and water pressure in the soil are expressed through their values in a state of complete stabilization. Therefore, it is conventionally assumed that the magnitude of the load does not change before the onset of this state, causing linear (relative to the load) deformations of the soil.

Thus, first, a plane problem of different modulus of the theory of a linearly deformable medium is solved. This problem is described by a system of partial differential equations. The solution is found by the finite element method with respect to displacements. Then, the steady-state and initial values of the stresses are determined, as well as the values of the maximum deviation of the total stress vector.

In the case of an isotropic medium, the initial fluid head function (H_o) satisfies the Laplace equation: $\Delta H_o = 0$. The first boundary value problem is posed and solved. Analytical expressions are obtained for the initial values of heads and stresses. With their help, one can select the optimal triangulation of the region for a given loading diagram and check the finite element solution.

The calculation results are presented as level lines of a function of two variables. The general view of the vertical stress function is in good agreement with the available experimental data.

It was found that the form of the transverse loading diagram has a significant effect on the degree of the stress state of the soil. At the same average contact pressures, the parabolic shape of the loading diagram, which is characteristic of tires with reduced internal air pressure, has the smallest effect on the soil.

The method can serve as the basis for predicting the degree of soil compaction and the intensity of rutting, as well as the environmental consequences of the operation of forest machines.

Keywords

Soil mechanics; Water-saturated soil; Environmental impact of vehicle; Forest vehicle; The first boundary value problem; The finite element method.

Introduction

The result of the harmful environmental impact of the skidder on the ground is soil compaction, destruction of sod cover, and rut formation. As shown by numerous observations in the USA, Canada and other countries, the use of a wheeled skidder in logging leads to soil compaction and, as a consequence, to a decrease in forest productivity. The operation of the machine causes compaction and destruction of the sod cover, which serves as the most important source of plant nutrition. There is a change in biogeochemical cycles, and seed germination worsens within the framework of natural reforestation.

Destruction of the upper sod layer, saturated with organic matter, occurs as a result of deepening the lugs and wheel slip. As the analysis of the impact of the wheel on the ground shows, the most important factors affecting the environmental consequences of movement are, on the one hand, the physical and mechanical properties of the soil, on the other hand, the ability of the wheel to realize the required traction force with minimal slipping and cause minimal soil compaction.

The most important today is the problem of reducing the impact of the vehicles on the ground and assessing its condition after the passage of the vehicle. Naturally, the question arises of identifying the factors affecting the deformation and compaction of the soil, and finding the mathematical relationships between them. The existing mathematical models of the interaction of the wheel with the ground are usually based on a one-dimensional stress distribution function over depth, which is obtained by processing the results of stamping tests [8]. With this approach, it is impossible to assess the plane and spatial phenomena, including the distribution of compaction zones under the wheel and edge effects that cause lateral uplift of the soil. In addition, the whole principle of constructing the model is based on the mechanical transfer of the results of stamp tests to the wheel rolling process, it does not reflect the dynamics of the phenomenon, and the complication of the model by the introduction of correction factors for the geometric parameters of the contact patch and the time of application of the load does not contribute to an increase in the accuracy of the solution, since their influence on the final result is nullified by averaging the load over the contact patch and the accuracy of obtaining soil characteristics. Therefore, it is necessary to look for new methods of constructing a mathematical model based on the theory of soil mechanics.

The basis for the construction of a mathematical model was a well-developed theory of soil mechanics. Its methods have been successfully applied in practice for a long time. There are proven methods for obtaining the required characteristics of soils and an extensive data on them.

The mathematical model, together with its software implementation, allows:

1) to judge the influence of the design features of the wheels and the nature of the vertical load on the distribution of stresses in the soil;

2) take into account the anisotropy of soil properties;

3) simulate movement on ice and swamp;

4) assess the ability and environmental impact of vehicle on soft ground;

5) predict the degree of soil compaction and the intensity of rutting during the operation of the forest machine.

1. Basic concepts of the physical and mechanical properties of soil

By their nature, soils are divided into two main classes: sands are products of mechanical destruction of basic rocks, and clays are products of chemical destruction of basic rocks. Sands and clays differ greatly in their physical and mechanical properties.

In nature, soils of mixed origin are usually found. They exhibit intermediate properties of sand and clay and are called, respectively, sandy loam, loam, etc.

All qualitative differences in soil properties are determined by the size and shape of the particles forming them. Of great importance in the manifestation of these properties is the water in the gaps between the particles. The gas in the soil (air, methane, water vapor) also strongly affects the properties of the soil.

Sands consist of particles having the shape of grains with a diameter of 0.5 - 2 mm (coarse sand) to 0.1 - 0.05 mm (fine sand) [3]. Clay particles are in the form of plates with a thickness of not more than 1 micron.

Let us introduce the notation.

V - some volume of soil;

V_p - pore volume;

V_s - volume of solid particles;

$V = V_p + V_s$;

$n = \frac{V_p}{V}$ - soil porosity;

$m = \frac{V_s}{V}$ - the volume of solid particles per unit volume of soil;

$n + m = 1$;

$\varepsilon = \frac{V_p}{V_s} = \frac{n}{m}$ - coefficient of porosity.

Compressibility of soils

Due to the low permeability of solid soil particles, compression deformation occurs mainly due to a change in porosity. The relationship between the coefficient of porosity ε and compressive stresses σ is obtained using uniaxial compression devices. The curve is shown in Fig.1.1.

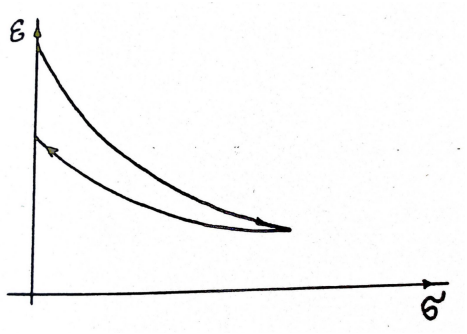

Fig.1.1: Compression curve

On small intervals of stresses change, it is approximated by a straight line

$$\varepsilon = -a\sigma + A \quad . \tag{1}$$

With a large number of loading and unloading, the soil becomes practically elastic.

Weakly compacted clays	0.10 - 0.01
Compacted clays	0.005 - 0.001

Compaction factors $a, cm^2/kg$ *(according to Florin)*

Sands	0.54 - 0.82
Compacted clays	0.67 - 1.2
Silt	1.00 - 3.00
Loams and clays	0.67 -1.00

Porosity coefficients ε *(according to Florin)*

Filtration properties of soils

The filtration rate is defined in soil mechanics as the flow rate of water through a unit of the geometrical area of the soil section. Darcy's law establishes a relationship between the filtration rate u and the fluid pressure gradient H :

$$u = -k\frac{\partial H}{\partial s} \quad ,$$

where k is the filtration coefficient [cm / s].

H is determined in hydraulics by the formula:

$$H = \frac{P}{\gamma} + z \quad , [\text{cm}]$$

where P is the pressure in the liquid [kg/cm^2],

γ - specific gravity of the liquid [kg/cm^3],

z - the height of this point above the zero mark [cm].

The actual speed of water relative to immobile soil grains is determined by the formula:

$$u_a = \frac{u}{n} \quad ,$$

where is n the porosity of the soil (see above).

In the case of movement of soil grains towards the liquid at a speed, v_a Darcy's law is written in the form:

$$u_a - v_a = -\frac{k}{n}\frac{\partial H}{\partial s} \Rightarrow u - \varepsilon v = -k\frac{\partial H}{\partial s} \quad . \qquad (2)$$

Sands	$10^{-2} - 10^{-3}$
Clays	$10^{-6} - 10^{-8}$

Filtration coefficient k , cm / s (according to Florin)

Understanding stresses in soil

Consider the case of deformation propagation in one plane. Let's select an elementary parallelepiped and call the ratio of the force acting on an elementary area to its area stress. Then, on the sections of the parallelepiped, inclined at different angles, we will get different values of stresses. The stress vector coincides in direction with the force vector and it can be decomposed into normal and tangential components: σ_n and τ (Fig. 1.2).

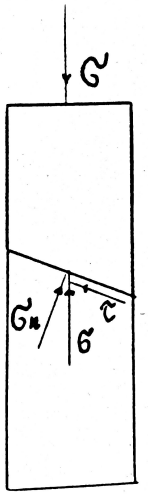

Fig.1.2 Plane stresses

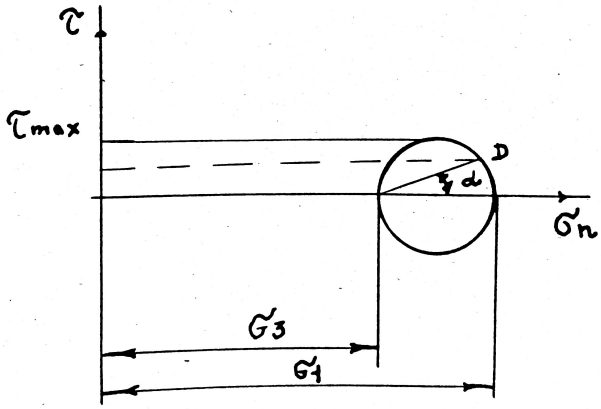

Fig.1.3 Mohr's circle

Let us introduce a rectangular coordinate system XoZ and denote the stresses acting along the oX and oZ axes, respectively, σ_x and σ_z .

Let only normal stress act in some section, and there is no tangential stress. This normal stress is called the main one. The largest and the smallest normal stresses acting in a given section are the main ones. They are denoted by σ_1 and σ_3 respectively.

It is convenient to determine the stress distribution in the sections of an elementary parallelepiped using Mohr's circles (Fig. 1.3).

It can be seen from the figure that in the section drawn at an angle α , the values of the normal and tangential stresses are determined by the coordinates of the point D on the circle. The maximum shear stress in absolute value is achieved at $\alpha=\pm\pi/4$.

The concept of soil strength

In soil mechanics, the main indicators of strength are considered to be the shear resistance of the soil. The maximum shear stress is determined from the equation:

$$\tau = c + \sigma_n \tan\varphi \quad , \tag{3}$$

where c is called adhesion, and φ is the angle of internal friction. For sands $c=0$, therefore

$\tau = \sigma_n \tan\varphi$. The φ angle for sands is a constant value , while for clays the cohesion and the angle of internal friction depend on the density and moisture. After preliminary compaction of the soil, an increase in adhesion and a decrease in the angle of internal friction are observed, this is due to an irreversible decrease in the coefficient of porosity ε , as a result of which the molecular forces of interaction between particles increase [6].

From equation (3), you can determine the straight lines, which are called the lines of destruction. For a given value σ_1 , construct a Mohr circle so that it touches these lines (Fig. 1.4).

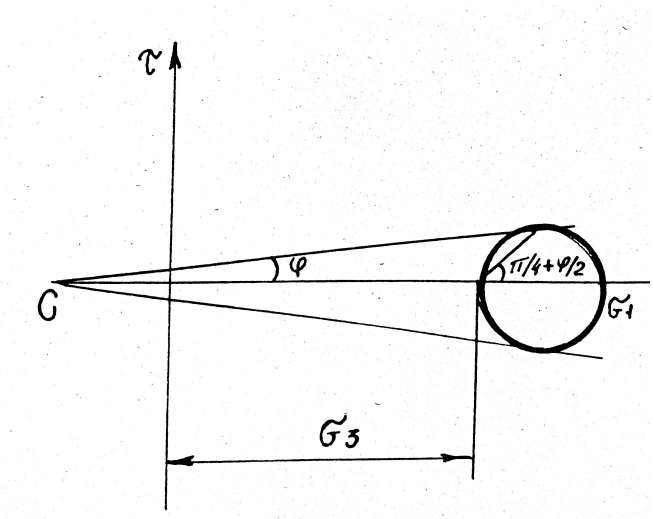

Fig.1.4 Plastic limit equilibrium

The slope of the fracture planes can now be determined. It makes an angle $\pi/4+\varphi/2$ to the line of action of the lowest principal stress. At this moment, the principal stresses satisfy the equation

$$\sigma_1 = 2c\sqrt{\lambda_\varphi} + \sigma_3\lambda_\varphi \quad , \tag{4}$$

where $\lambda_\varphi = \tan^2(\pi/4+\varphi/2)$, and the soil massif is in a state of so-called plastic limiting equilibrium [9]. The effect of the hydrostatic pressure of water in the pores of the soil should also be taken into account, therefore, the so-called effective stress, which is perceived by the skeleton of the soil, should be substituted in formulas (3) and (4), and their values are less than the actual stresses by the value of the pore pressure of water. The sine of the largest deviation of the total stress vector can be represented as:

$$\sin\theta_{max} = \frac{\sqrt{(\sigma_x - \sigma_z)^2 + 4\tau_{xz}^2}}{\sigma_z + \sigma_x + 2c/\tan\varphi} \quad .$$

Deformation modulus and Poisson's ratio

When compressing a soil sample in a compression device, transverse deformations of the soil are impossible. In this case, the lateral pressure coefficient ζ is determined by the formula: $\zeta = \frac{\sigma_x}{\sigma_z}$. In soil mechanics, it is assumed that porosity depends only on the sum of the principal stresses, and not on

their ratios. This assumption is based on the approximation of the real stress-strain curve by a straight line with sufficient accuracy for practical calculations. Because of this, we write formula (1) for the case of a biaxial stress state (plane problem):

$$\varepsilon = -a\frac{\theta}{1+\zeta} + A \quad , \tag{5}$$

here $\theta = \sigma_x + \sigma_z$ is the sum of the principal stresses.

The deformation modulus $E(\varepsilon)$ is determined in soil mechanics from the expression:

$$de_x = \frac{d\sigma_x - \nu d\sigma_z}{E(\varepsilon)} \quad ,$$

where σ_x and σ_z is the increment in stresses, that caused de_x - the strain increment along the oX axis.

Poisson's ratio ν is defined through the lateral pressure coefficient ζ : $\nu = \frac{\zeta}{1+\zeta}$.

If we take the dependence $\varepsilon = \varepsilon(\theta)$ as linear, for example, in the form (5), we obtain

$$E = \frac{\beta(1+\varepsilon)}{a} \quad ,$$

where $\beta = \frac{(1-\zeta)(1+2\zeta)}{(1+\zeta)}$.

Sands	0.40-0.42
Clays	0.70-0.75

Lateral pressure coefficient (according to Florin)

The above expressions for the deformation moduli make it possible, in the case of a nonlinear relationship between stresses and strains, to determine the modulus value for any given stress state. However, in many cases it is more convenient to use the so-called average deformation modulus

$E_{avg} = \frac{\beta(1+\varepsilon_1)}{a}$, where ε_1 is the initial porosity coefficient.

It was shown (N.M. Gersevanov) the constancy of E_{avg} for plastic soils in a small range of load variation, which indicates a linear relationship between stresses in the skeleton and its deformations, and this shows that the formulas of the theory of elasticity are applicable to the calculations of stresses and deformations in the soil skeleton.

In conclusion, let us consider the case of applying a vertical load along the rectilinear boundary of a linearly deformed medium. In this case [10]:

$$\sigma_x=\frac{1}{2}\theta+\frac{1}{2}z\frac{\partial\theta}{\partial z}$$

$$\sigma_z=\frac{1}{2}\theta-\frac{1}{2}z\frac{\partial\theta}{\partial z} \qquad (6)$$

$$\tau_{xz}=-\frac{1}{2}z\frac{\partial\theta}{\partial x}$$

The stress components are determined by the formulas:

$$\sigma_x=\lambda e+\nu\varepsilon_x$$

$$\sigma_z=\lambda e+\nu\varepsilon_z \quad ,$$

where $\varepsilon_x=\frac{\partial u_1}{\partial x}$, $\varepsilon_z=\frac{\partial u_3}{\partial z}$, $\lambda=\frac{\nu E}{(1+\nu)(1-2\nu)}$, $e=\varepsilon_x+\varepsilon_z$,

u_1 и u_3 - displacement components.

$$\tau_{xz}=\nu\gamma_{xz} \quad ,$$

where $\gamma_{xz}=\frac{\partial u_1}{\partial z}+\frac{\partial u_3}{\partial z}$.

For a general model of a linearly deformable medium, the stresses in the soil skeleton must satisfy the equations [10]:

$$\frac{\partial\sigma_x}{\partial x}+\frac{\partial\tau_{xz}}{\partial z}+X=0 \qquad (7)$$

$$\frac{\partial\tau_{xz}}{\partial x}+\frac{\partial\sigma_z}{\partial z}+Z=0 \quad , \qquad (8)$$

where X и Z - components of volumetric forces,

along with the equation

$$\Delta(\sigma_x+\sigma_z)=-\frac{1}{1-\nu}\left(\frac{\partial X}{\partial x}+\frac{\partial Z}{\partial z}\right) \quad , \qquad (9)$$

where ν - коэффициент Пуассона ;

Δ - оператор Лапласа.

2. Mathematical formulation of the compaction problem

2.1. The Simplest One-Dimensional Compaction Problem

Key assumptions:

a) We consider models of a two-component soil consisting of solid particles and water filling its pores. This model is called soil mass. “The question may arise: in what cases, in practice, are we dealing with a soil mass? ... As for the ground lying above the groundwater level, in the vast majority of cases it is a soil mass, that is, one in which all voids are filled with water due to the capillary rise of water in the fine pores of the soil. In clays, the length of the capillary rise of water can reach a height of over 300 m above the groundwater level.

In order to judge whether we have a soil mass above the groundwater level, we can be guided by the following signs: in all cases when the soil is in a fluid, plastic and semi-solid state, we are dealing with a soil mass. Only when the soil passes from a semi-solid state to a solid state does air penetrate into the pores of the soil and partially fill the voids of the soil skeleton. The transition from solid to solid is characterized by a sharp change in the color of the soil. … To determine the condition of the soil, i.e. whether it is fluid, plastic or semi-solid, there are fully developed laboratory methods ... ”(N.M. Gersevanov, [2, p. 145]).

b) the change in porosity occurs only due to the dense packing of soil particles;

c) the filtration coefficient does not depend on the stress state.

Basic equations

1. Equations of continuity for solid and liquid soil components.

$$\frac{\partial u_z}{\partial z}+\frac{\partial n}{\partial t}=0 \quad , \tag{1}$$

$$\frac{\partial v_z}{\partial z}+\frac{\partial m}{\partial t}=0 \quad , \tag{2}$$

here, as before, v_z u_z and are the flow rates of the solid and liquid components along the oZ axis. Adding equations (1), (2) and taking into account equality $n+m=1$, we obtain

$$\frac{\partial u_z}{\partial z}+\frac{\partial v_z}{\partial z}=0 \quad . \tag{3}$$

2. Darcy's dependency.

$$u_z-\varepsilon v_z=-k\frac{\partial H}{\partial z} \quad . \tag{4}$$

3. Equilibrium equation.

Let σ - stress in the soil skeleton; p - pressure in water; σ^* and p^* - the corresponding values in a state of complete stabilization.

$$\sigma + p = \sigma^* + p^* \quad . \tag{5}$$

That is the sum of stress and pressure is a constant.

Differentiate (4) by z :

$$\frac{\partial u_z}{\partial z} - \frac{\partial \varepsilon}{\partial z} v_z - \varepsilon \frac{\partial v_z}{\partial z} = -\frac{\partial}{\partial z}\left(k \frac{\partial H}{\partial z}\right) \quad ,$$

considering (3):

$$v_z \frac{\partial \varepsilon}{\partial z} + (1+\varepsilon) \frac{\partial v_z}{\partial z} = \frac{\partial}{\partial z}\left(k \frac{\partial H}{\partial z}\right) \quad .$$

Further, taking into account (2) and the relationship between ε and m from Section 1, we obtain:

$$\frac{\partial v_z}{\partial z} = -\frac{\partial m}{\partial t} = -\frac{\partial}{\partial t}\left(\frac{1}{1+\varepsilon}\right) = \frac{1}{(1+\varepsilon)^2} \frac{\partial \varepsilon}{\partial t} \quad ;$$

$$v_z \frac{\partial \varepsilon}{\partial z} + (1+\varepsilon) \frac{\partial v_z}{\partial z} = \frac{\partial}{\partial z}\left(k \frac{\partial H}{\partial z}\right) \quad .$$

Further, as shown in [4],

$$v_z \frac{\partial \varepsilon}{\partial z} = o\left(\frac{\partial \varepsilon}{\partial t}\right)$$

and the error from replacement $[1+\varepsilon(t,z)]$ by $[1+\varepsilon(t,z)]$ (ε is the average porosity in the considered compaction range) is less than the error of the laboratory determination of the filtration coefficient k .

In view of the above

$$\frac{\partial \varepsilon}{\partial z} = (1+\varepsilon) \frac{\partial}{\partial z}\left(k \frac{\partial H}{\partial z}\right)$$

$$\frac{\partial \varepsilon}{\partial t} = \frac{d\varepsilon}{d\sigma} \frac{\partial \sigma}{\partial t} = -a\left(-\frac{\partial p}{\partial t}\right) = a\gamma \frac{\partial H}{\partial t} \quad .$$

Here we used equation (1) from Section 1 and equilibrium equation (5). We will finally write down

$$\frac{\partial H}{\partial t} = \frac{(1+\varepsilon)}{a\gamma} \frac{\partial}{\partial z}\left(k \frac{\partial H}{\partial z}\right) \quad . \tag{6}$$

The resulting equation is equivalent in form to the equation of heat conduction and diffusion.

Next, the initial and boundary conditions are assigned:

$t=0,\ H=H(Z)$;

$t>0,\ z=0:\ H=\lambda(t),\ z=z^*:\ H=\mu(t)$.

Example. Let the distributed load $q:\ H_o=q/\gamma$ be instantaneously applied at the initial moment $t=0$. If the layers $z=0$ and $z=z^*$ are also permeable, then when $t>0$:

$z=0,\ H=0;\ z=z^*,\ H=0$,

For waterproof layers $\frac{\partial H}{\partial z}=0$.

The solution of equation (6) together with the given initial and boundary conditions is found by known methods, for example, by the method of separation of variables (by the Fourier method). The stress distribution $\sigma(z,t)$ is determined from equation (5):

$$\sigma+p=const=q$$

$$\sigma=q-p=q-\gamma H \quad .$$

The amount of compaction can be found by the formula:

$$s(t,h)=\int_o^h e_z(t,z)\,dz \quad ,$$

where e_z is the compaction of the layer with the coordinate z , according to the results of Section 1

$$e_z=\frac{a}{1+\varepsilon}\sigma \quad ;$$

h - active compaction depth, can be determined in the following way:

make up a sequence $(h_k),k=0,1,2...$ and determine h_l from the condition:

$$\frac{|s(t,h_{l-1})-s(t,h_l)|}{s(t,h_l)}\le\delta$$

Where δ is the specified accuracy. Thus, the problem of compaction in the one-dimensional case can

be considered solved.

2.2. Plane and spatial problems of compaction

The assumptions are the same as in the previous paragraph. First, consider the planar compaction problem (XoZ plane).

Basic equations.

1. Equations of continuity

$$\frac{\partial u_x}{\partial x}+\frac{\partial u_z}{\partial z}+\frac{\partial n}{\partial t}=0 \tag{1}$$

$$\frac{\partial v_x}{\partial x}+\frac{\partial v_z}{\partial z}+\frac{\partial m}{\partial t}=0 \quad . \tag{2}$$

Add equations (1), (2)

$$\frac{\partial (u_x+v_x)}{\partial x}+\frac{\partial (u_z+v_z)}{\partial z}=0 \quad . \tag{3}$$

2. Darcy's dependence

$$u_x-\varepsilon v_x=-k\frac{\partial H}{\partial x} \tag{4}$$

$$u_z-\varepsilon v_z=-k\frac{\partial H}{\partial z} \quad . \tag{5}$$

3. Equilibrium equations

$$\sigma_x+p=\sigma_x^*+p^* \tag{6}$$

$$\sigma_z+p=\sigma_z^*+p^* \tag{7}$$

$$\tau_{xz}=\tau_{xz}^* \quad . \tag{8}$$

Here τ_{xz} are the shear stresses. It is assumed that the tangential load is instantly perceived by the skeleton and is not transmitted to the water.

Differentiate (4) by x , (5) by z and add up:

$$\frac{\partial u_x}{\partial x}+\frac{\partial u_z}{\partial z}-\varepsilon\left(\frac{\partial v_x}{\partial x}+\frac{\partial v_z}{\partial z}\right)=-\left[\frac{\partial}{\partial x}\left(k\frac{\partial H}{\partial x}\right)+\frac{\partial}{\partial z}\left(k\frac{\partial H}{\partial z}\right)\right] \quad .$$

Comment. Discarded terms $\frac{\partial \varepsilon}{\partial z}v_z$ and $\frac{\partial \varepsilon}{\partial x}v_x$.

Taking into account (3), we obtain

$$(1+\varepsilon)\left(\frac{\partial v_x}{\partial x}+\frac{\partial v_z}{\partial z}\right)=\frac{\partial}{\partial x}\left(k\frac{\partial H}{\partial x}\right)+\frac{\partial}{\partial z}\left(k\frac{\partial H}{\partial z}\right) \quad ,$$

where the value $1+\varepsilon$ is a constant (see section 2.1).
Further, from (2) we have

$$\frac{\partial v_x}{\partial x}+\frac{\partial v_z}{\partial z}=-\frac{\partial m}{\partial t}=\frac{1}{(1+\varepsilon)^2}\frac{\partial \varepsilon}{\partial t} \quad ,$$

taking this into account, we get

$$\frac{\partial \varepsilon}{\partial t}=(1+\varepsilon)\left[\frac{\partial}{\partial x}\left(k\frac{\partial H}{\partial x}\right)+\frac{\partial}{\partial z}\left(k\frac{\partial H}{\partial z}\right)\right] \quad . \tag{9}$$

Next, we use equation (5) from Section 1.1. We have

$$\frac{\partial \varepsilon}{\partial t}=\frac{d\varepsilon}{d\sigma}\frac{\partial \sigma}{\partial t}=-\frac{a}{1+\xi}\frac{\partial \theta}{\partial t} \quad .$$

From equations (6) and (7) we obtain

$$\theta=\sigma_x+\sigma_z=\theta^*=\sigma_x^*+\sigma_z^*-2(p-p^*)$$

so

$$\frac{\partial \theta}{\partial t}=-2\frac{\partial p}{\partial t}=-2\gamma\frac{\partial H}{\partial t} \quad .$$

Let us finally write equation (9) in the form:

$$\frac{\partial H}{\partial t}=\frac{(1+\varepsilon)(1+\xi)}{2\gamma a}\left[\frac{\partial}{\partial x}\left(k\frac{\partial H}{\partial x}\right)+\frac{\partial}{\partial z}\left(k\frac{\partial H}{\partial z}\right)\right] \quad . \tag{10}$$

Reasoning quite similarly in the case of a triaxial stress state, we arrive at the equation:

$$\frac{\partial H}{\partial t}=\frac{(1+\varepsilon)(1+2\xi)}{3\gamma a}\left[\frac{\partial}{\partial x}\left(k\frac{\partial H}{\partial x}\right)+\frac{\partial}{\partial y}\left(k\frac{\partial H}{\partial y}\right)+\frac{\partial}{\partial z}\left(k\frac{\partial H}{\partial z}\right)\right] \quad . \tag{11}$$

Let us assume that the filtration coefficient k does not change during the compaction process. Then we have:

$$\frac{\partial H}{\partial t} = K \Delta H \quad . \tag{12}$$

Where Δ is the Laplace operator,

$K = \frac{(1+\varepsilon)(1+\xi)}{2\gamma a} k$ - for a plane problem

405

$K = \frac{(1+\varepsilon)(1+2\xi)}{3\gamma a} k$ - for a spatial problem.

Initial conditions

Note that the initial heads distribution function H_o satisfies the Laplace equation

$$\Delta H_o = 0 \quad . \tag{13}$$

410

This equation is a consequence of the fact that at the initial moment of load application

$$\frac{\partial v_x}{\partial x} = \frac{\partial v_y}{\partial y} = \frac{\partial v_z}{\partial z} = 0 \quad .$$

415 We find the initial pressure distribution from (6) and (7):

in the case of the plane problem

$$P_o = \frac{1}{2}\theta_o^* + P_o^* \quad , \tag{14}$$

for a spatial task

$$P_o = \frac{1}{3}\theta_o^* + P_o^* \quad . \tag{15}$$

Here, as before, θ_o^* denotes the sum of normal stresses in a stabilized state, P_o^* is the final pressure

420 distribution. We accept further $P_o^* = 0$.

Thus, to determine the initial distribution of the pressure, it is necessary to solve problems (7), (8) and (9) of the theory of elasticity (Section 1).

The initial stress distribution is determined from (6), (7), (14), (15)

For a planar problem

425

$$\sigma_{xo} = \frac{1}{2}(\sigma_x^* - \sigma_z^*)$$

$$\sigma_{zo} = \frac{1}{2}(\sigma_z^* - \sigma_x^*)$$

$$\tau_{xzo} = \tau_{xz}^* \quad .$$

For a spatial problem

$$\sigma_{xo}=\sigma_x^*-\frac{1}{3}\theta_o^*$$

$$\sigma_{yo}=\sigma_y^*-\frac{1}{3}\theta_o^*$$

$$\sigma_{zo}=\sigma_z^*-\frac{1}{3}\theta_o^*$$

$$\tau_{xzo}=\tau_{xz}^*,\quad \tau_{xyo}=\tau_{xy}^*,\quad \tau_{yzo}=\tau_{yz}^* \quad .$$

Border conditions

On the permeable sections of the boundary surface, the values of the pressure function are equal to zero: $H=0,\ x\in\Gamma$. In watertight areas, the pressure gradient value is zero:

$$\frac{\partial H}{\partial n}=0,\ x\in\Gamma \quad .$$

In addition, in the case of compaction of heterogeneous soil, the conjugation conditions must be met at the border of adjacent media:

$$H_1(x,t)|_S=H_2(x,t)|_S \quad ;$$

$$k_1\left(\frac{\partial H_1}{\partial n}\right)=k_2\left(\frac{\partial H_2}{\partial n}\right) \quad .$$

Example. The plane problem of compaction of isotropic soil with an arbitrary vertical load. We find the initial stress distribution from equation (6) in Section 1 and from equations (6), (7), (8):

$$\begin{aligned}\sigma_{xo}&=\frac{1}{2}(\sigma_x^*-\sigma_z^*)=\frac{1}{2}z\frac{\partial\theta^*}{\partial z}=z\frac{\partial P_o}{\partial z}\\ \sigma_{zo}&=\frac{1}{2}(\sigma_z^*-\sigma_x^*)=-z\frac{\partial P_o}{\partial z}\\ \tau_{xzo}&=\tau_{xz}^*=\frac{1}{2}z\frac{\partial\theta^*}{\partial x}=-z\frac{\partial P_o}{\partial z}\end{aligned} \quad . \qquad (16)$$

To determine P_o , it is necessary to solve the following problem:

$$\Delta P_o=0 \quad ,$$

$z=0,\ x\in D \quad P_0=q(x)$ - given load,

$$\begin{aligned}&x\notin D \quad P_o=0;\\ &x\to\pm\infty,\quad z\to\pm\infty,\quad P_o=0\end{aligned} \quad . \qquad (17)$$

Consider a more general first boundary value problem:

$$\begin{matrix} Lu=-f(M),\ \ (M\in D) \\ u|_S=\varphi(M) \end{matrix} \quad . \tag{18}$$

In the original problem

$$u\equiv H,\quad Lu=\Delta u=\frac{\partial^2 u}{\partial x^2}+\frac{\partial^2 u}{\partial z^2}\ \ ;$$

$$f(M)=f(x,z)=0,\ (M\in D)\ \ ;$$

455
$$\varphi(M)=\varphi(x,z)\quad \equiv \quad \begin{cases} 0,\ z=0,\ x\notin[-a,a] \\ q(x),\ z=0,\ x\in[-a,a] \\ 0,\ z\to+\infty,\ x\to\pm\infty \end{cases},$$

where $q(x)=\gamma\varrho(x)$ is the diagram of the load distribution, 2a is the contact width (Figure 2.1).

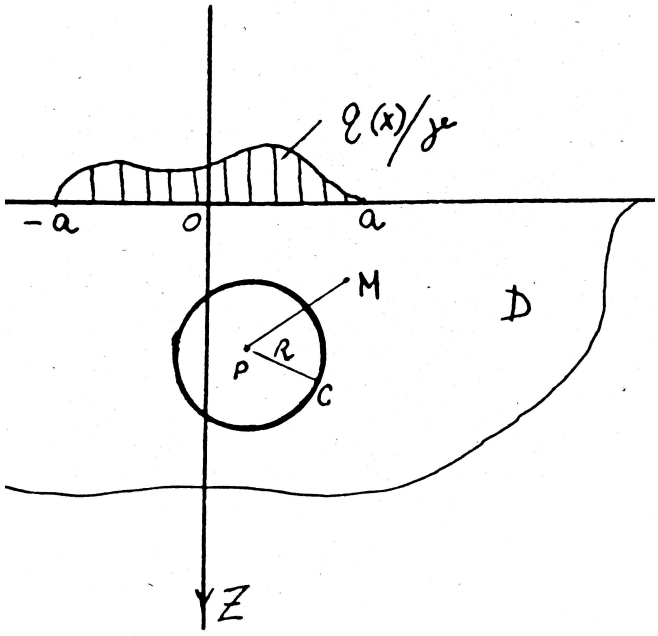

Fig.2.1 On the definition of the Green's function

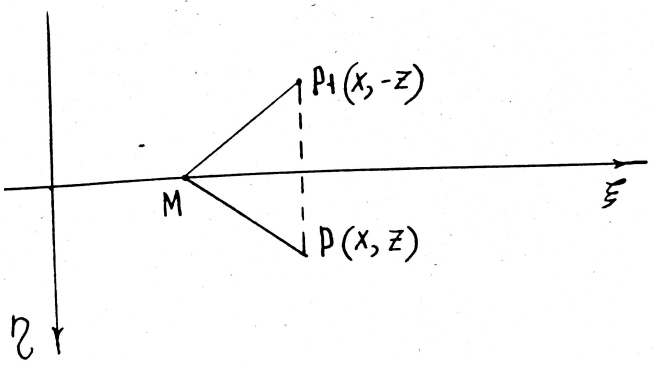

Fig.2.2 Reflection method

460

To solve problem (18), the method of Green's functions is used, the solution has the form [5]:

$$u(P)=-\int_S \varphi\frac{\partial G}{\partial n}dS_M$$

where $G=G(M,P)$ is the solution to an equation of a special form:

$$\begin{cases} \Delta G = -\delta(M, P) \ \ (M \in D) \\ G|_S = 0 \end{cases} . \tag{19}$$

Here $\delta(M, P)$ is the Dirac δ - function. Solution (19) is presented in the form:

$$G(M, P) = \psi(\Gamma_{MP}) + V(M, P) \ ,$$

where V is harmonious at D (i.e. $\Delta V = 0, M \in D$), and $\psi(\Gamma_{MP})$ has a singularity at the point P and at $\Gamma_{MP} = 0$

$$\Delta \psi = -\delta(M, P) \ . \tag{20}$$

We integrate (20)

$$\int_{S_P^R} \Delta \psi \, ds = -1 \quad (\ \delta \ \text{- function property}).$$

Using Green's formula, we pass to the integral over a circle centered at the point P of radius R (see Figure 2.1):

$$\oint_C \frac{\partial \psi}{\partial n} ds = \oint_C \frac{d\psi}{dr} ds = \frac{d\psi}{dr}|_R \cdot 2\pi R = -1$$
$$d\psi(R) = -\frac{1}{2\pi}\frac{dR}{R} \Rightarrow \psi(R) = -\frac{1}{2\pi}\ln\frac{1}{R} \ .$$
$$\Rightarrow G(M, P) = \frac{1}{2\pi}\ln\left(\frac{1}{\Gamma_{MP}}\right) + V(M, P)$$

For our case $V(M, P)$ is determined by the method of reflections (Figure 2.2).

Due to the fact that on the boundary of the half-plane $G(M, P) = 0$, it follows that

$V(M, P) = -\frac{1}{2\pi}\ln\left(\frac{1}{\Gamma_{MP_1}}\right)$ is a harmonic function $\forall M \in D$.

$$\Rightarrow G(M, P) = \frac{1}{2\pi}\ln\left(\frac{1}{\Gamma_{MP}}\right) - \frac{1}{2\pi}\ln\left(\frac{1}{\Gamma_{MP_1}}\right) \ ,$$

or in coordinates $x, z, \xi, \eta : (M(\xi, \eta), P(x, z))$:

$$G(M, P) = \frac{1}{2\pi}\ln\left(\frac{1}{\sqrt{(x-\xi)^2 + (z-\eta)^2}}\right) - \frac{1}{2\pi}\ln\left(\frac{1}{\sqrt{(x-\xi)^2 + (z+\eta)^2}}\right)$$

$$\Rightarrow u(P) = -\int_a^{-a} \varrho(\xi)\frac{\partial G}{\partial \eta}|_{\eta=0} d\eta \ , \text{ and it remains to find}$$

$$\frac{\partial G}{\partial \eta}|_{\eta=0} = \frac{1}{2\pi}\ln\left(\frac{2z}{(x-\xi)^2 + z^2}\right) \ .$$

Thus, the solution (18) is:

$$H_o(x,z)=\frac{1}{\pi}\int_a^{-a}\varrho(\xi)\frac{z}{(x-\xi)^2+z^2}d\xi \quad .$$

For the original problem, this is equivalent to the following expression:

$$H_o(x,z)=\frac{1}{\pi}\int_a^{-a}\varrho(\xi)\frac{z}{(x-\xi)^2+z^2}d\xi \quad .$$

So found in the initial pressure distribution:

$$P_o(x,z)=\frac{\gamma}{\pi}\int_a^{-a}\varrho(\xi)\frac{z}{(x-\xi)^2+z^2}d\xi \quad ,$$

where $\varrho(\xi)=\frac{q(\xi)}{\gamma}$, that is, you can rewrite

$$P_o(x,z)=\frac{1}{\pi}\int_a^{-a}q(\xi)\frac{z}{(x-\xi)^2+z^2}d\xi \quad . \qquad (21)$$

We find the initial stress distribution by the formulas (16):

$$\sigma_{xo}=z\frac{\partial P_o}{\partial z}=\frac{z}{\pi}\int_{-a}^{a}q(\xi)\frac{(x-\xi)^2-z^2}{[(x-\xi)^2+z^2]^2}d\xi$$

$$\sigma_{zo}=-\sigma_{xo} \quad . \qquad (22)$$

$$\tau_{xzo}=-z\frac{\partial P_o}{\partial z}=\frac{1}{\pi}\int_{-a}^{a}q(\xi)\frac{2z(x-z)}{[(x-\xi)^2+z^2]^2}d\xi$$

The distribution of initial stresses and pressures for an arbitrary vertical load is shown in Figures 2.3 and 2.4.

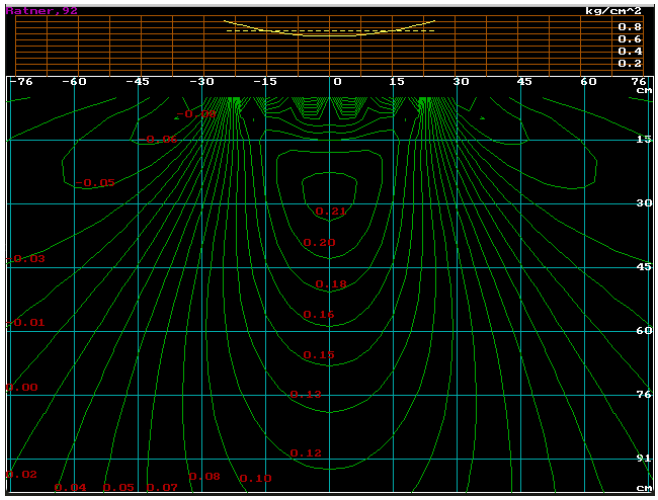

Fig.2.3 The distribution of initial stresses $(\sigma_{zo}, kg/cm^2)$ *in a homogeneous environment*

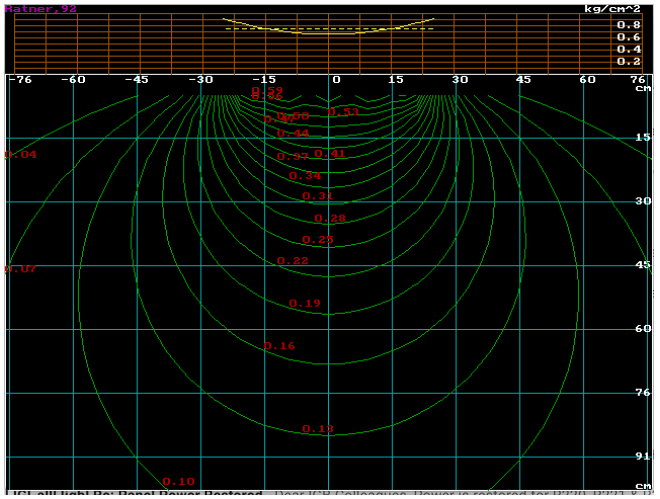

Fig.2.4 The distribution of initial pressures $(P_o, kg/cm^2)$ *in a homogeneous environment*

3. Finite-element solution of a multimodular problem of the theory of elasticity

505 The initial conditions of problem (12) in Section 2 are expressed in terms of the steady-state stress distribution, the definition of which is devoted to this section.

Earlier it was indicated (Section 1) that the formulas of the theory of elasticity are formally applicable to the calculation of stresses and strains in the soil skeleton, although in essence it means the presence of not elastic, but a linear relationship between stresses and deformations.

510 Select a rectangular area on the half-plane and triangulate it (Figure 3.1).

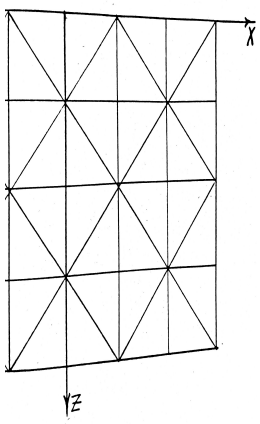

Fig.3.1 Area triangulation

Consider the four types of triangles used in the partition. The nodes are numbered clockwise (Figure 3.2).

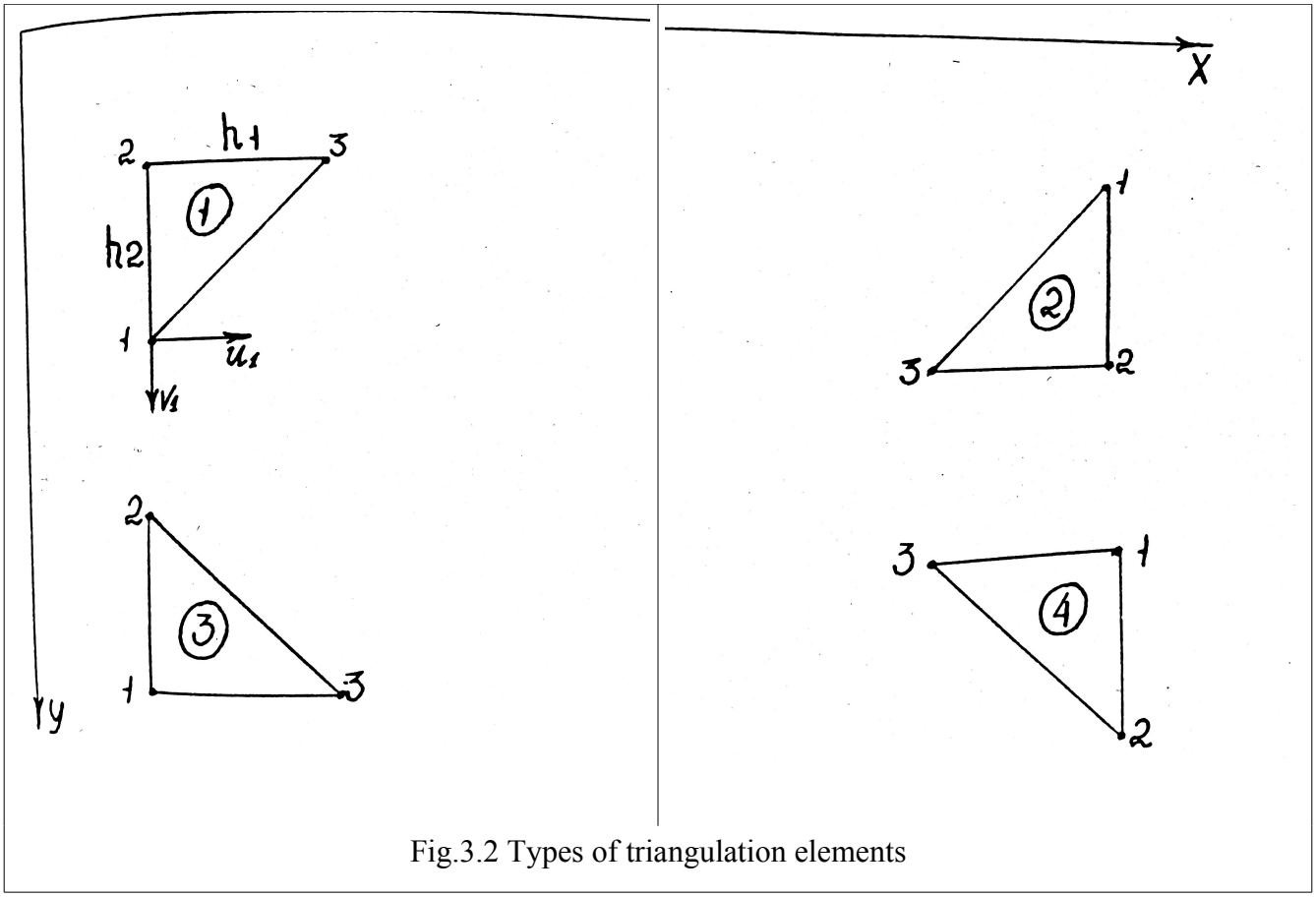

Fig.3.2 Types of triangulation elements

We denote the movement of the i-th node of a separate element through u_i and v_i . The displacements of the nodes belonging to the vertical boundaries of the half-plane are set to zero.

The displacements of element points are expressed in terms of nodal displacements:

$$U_N = \Phi U \quad . \tag{1}$$

Where $U_N = \begin{bmatrix} U(x,y) \\ V(x,y) \end{bmatrix}$ - the vector of displacements;

$\Phi = \begin{bmatrix} \varphi_1 0 \varphi_2 0 \varphi_3 0 \\ \varphi_1 0 \varphi_2 0 \varphi_3 0 \end{bmatrix}$ - shape matrix;

$\varphi_{1,} \varphi_{2,} \varphi_3$ - form functions on an element;

$U = \left[u_{1,} v_{1,} u_{2,} v_{2,} u_{3,} v_3 \right]^T$ - vector of nodal values of displacements on the element.

We carry out a functional expressing the potential energy of a deformed body:

$$I = \sum_{e=1}^{e=l} t_e \int_{\Omega_e} \frac{1}{2} \varepsilon^T \sigma \, d\Omega_e - \sum_{e=1}^{e=l} t_e \int_{\Gamma_e} U_N{}^T Q \, d\Gamma_e \quad . \tag{2}$$

Here the contributions are summed over l - elements, each of them with thickness t_e , area Ω_e ;

$\varepsilon = (\varepsilon_x, \varepsilon_y, \gamma_{xy})^T$ - deformation vector,

$\sigma = (\sigma_x, \sigma_y, \tau_{xy})^T$ - stress vector,

$Q = (q_x, q_y)^T$ is the vector of the distributed load applied to the boundary Γ_e of the boundary element e .

The relationship between stresses and deformation is expressed by Hooke's law [10]:

$$\sigma = D\varepsilon \quad . \tag{3}$$

Here D is the elasticity matrix of the element:

$$D = \frac{E}{1-\nu^2}\begin{bmatrix} 1 & \nu & 0 \\ \nu & 1 & 0 \\ 0 & 0 & (1-\nu)/2 \end{bmatrix} ,$$

where E is the modulus of deformation on the element,

ν - Poisson's ratio on the element.

The relationship between displacement and deformation is expressed by the formula [10]:

$$\varepsilon = \begin{bmatrix} \frac{\partial u}{\partial x} \\ \frac{\partial v}{\partial y} \\ \frac{\partial u}{\partial x} + \frac{\partial v}{\partial y} \end{bmatrix}$$

or, taking into account (1), we write

$$\varepsilon = B \cdot U \tag{4}$$

where

$$B = \begin{bmatrix} \frac{\partial}{\partial x} & 0 \\ 0 & \frac{\partial}{\partial y} \\ \frac{\partial}{\partial x} + \frac{\partial}{\partial y} \end{bmatrix} \cdot \Phi = \begin{bmatrix} \frac{\partial \varphi_1}{\partial x} & 0 & \frac{\partial \varphi_2}{\partial x} & 0 & \frac{\partial \varphi_3}{\partial x} & 0 \\ 0 & \frac{\partial \varphi_1}{\partial y} & 0 & \frac{\partial \varphi_2}{\partial y} & 0 & \frac{\partial \varphi_3}{\partial x} \\ \frac{\partial \varphi_1}{\partial y} & \frac{\partial \varphi_1}{\partial x} & \frac{\partial \varphi_2}{\partial y} & \frac{\partial \varphi_2}{\partial x} & \frac{\partial \varphi_3}{\partial y} & \frac{\partial \varphi_3}{\partial x} \end{bmatrix} .$$

We accept the functions of the shape of the element as linear and equal on the element to its barycentric coordinates, and outside the element to zero:

$$\varphi_i = \frac{a_i x + b_i y + c_i}{2S}, i = 1,2,3 \quad .$$

Where S is the area of the element,

$$\left.\begin{aligned} a_1 &= y_2 - y_3 \\ b_1 &= x_3 - x_2 \\ c_1 &= x_2 y_3 - x_3 y_2 \end{aligned}\right\} \quad . \tag{5}$$

The coefficients $a_2, a_3, b_2, b_3, c_2, c_3$ are determined through the cyclic permutation of the indices in (5). Then the matrix B will take the form:

$$B = \frac{1}{2S}\begin{bmatrix} a_1 & 0 & a_2 & 0 & a_3 & 0 \\ 0 & b_1 & 0 & b_2 & 0 & b_3 \\ b_1 & a_1 & b_2 & a_2 & b_3 & a_3 \end{bmatrix} \quad .$$

Let's rewrite (2) taking into account (1), (3), (4):

$$I = \sum_{e=1}^{e=l} t_e \int_{\Omega_e} \frac{1}{2} U^T B^T D \cdot B \cdot U \, d\Omega_e - \sum_{e=1}^{e=l} t_e \int_{\Gamma_e} U^T \Phi Q \, d\Gamma_e \quad . \tag{6}$$

A finite-element solution provides a minimum to functional (6) on the class of functions from a finite-dimensional space with a basis $(\varphi_e)_{e=1}^{e=l}$, $\varphi_e = (\varphi_1^e, \varphi_2^e, \varphi_3^e)$ [1].

The necessary condition for the minimum of functional (6):

$$\sum_{e=1}^{e=l} \frac{\partial I^e}{\partial U} = \sum_{e=1}^{e=l} \int_{\Omega_e} t_e B^T D \cdot B \cdot U \, d\Omega_e - \sum_{e=1}^{e=l} \int_{\Gamma_e} t_e \Phi Q \, d\Gamma_e = 0, \quad .$$
$$e = 1,2,\ldots,l$$

Therefore, we find the solution from the system of linear equations:

$$K_f \cdot U_f = F_f \quad . \tag{7}$$

Here U_f is the global vector of nodal values:

$$U_f = (U^1, U^2, \ldots, U^l)^T \quad ,$$

K_f - a global stiffness matrix composed of element stiffness matrices (the so-called local stiffness matrices) K^e :

$$K^e = \int_{\Omega_e} t_e B^T D B U \, d\Omega_e \quad ,$$

F_f - global load vector, composed of load vectors of elements:

$$F_f^e = \int_{\Gamma_e} t_e \Phi^T Q \, d\Gamma_e \quad .$$

Consider a boundary element with a distributed vertical load applied to it (Figure 3.3).

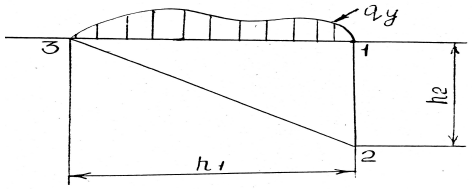

Fig.3.3 Scheme of load application to the boundary element

In the case of linear linear functions of the form, we have on the boundary:

$$\varphi_2 = 1 - \frac{s}{h_1} \quad , \quad \varphi_3 = \frac{s}{h_1}$$

$$F_f^e = t_e \int_0^{h_1} (0 \;\; 0 \;\; 0 \;\; \varphi_2 q_y \;\; 0 \;\; \varphi_3 q_y)^T \, dS \quad . \tag{8}$$

575

Here are the specific values of the matrices and coefficients. Let's denote for convenience $\xi = \frac{h_1}{h_2}$.

The matrix B^e

Elements of the 1st type

$$B^{(1)} = \begin{bmatrix} 0 & 0 & -1/\xi & 0 & 1/\xi & 0 \\ 0 & \xi & 0 & -\xi & 0 & 0 \\ \xi & 0 & -\xi & -1/\xi & 0 & 1/\xi \end{bmatrix}$$

580

Elements of the 2nd type

$$B^{(2)} = \begin{bmatrix} 0 & 0 & 1/\xi & 0 & -1/\xi & 0 \\ 0 & -\xi & 0 & \xi & 0 & 0 \\ -xi & 0 & \xi & 1/\xi & 0 & -1/\xi \end{bmatrix}$$

Elements of the 3rd type

585

$$B^{(3)} = \begin{bmatrix} -1/\xi & 0 & 0 & 0 & 1/\xi & 0 \\ 0 & \xi & 0 & -\xi & 0 & 0 \\ \xi & -1/\xi & -xi & 0 & 0 & 1/\xi \end{bmatrix}$$

Elements of the 4th type

$$B^{(4)} = \begin{bmatrix} 1/\xi & 0 & 0 & 0 & -1/\xi & 0 \\ 0 & -\xi & 0 & \xi & 0 & 0 \\ -xi & 1/\xi & xi & 0 & 0 & -1/\xi \end{bmatrix} \quad .$$

The Matrix K^e

We denote $d=\frac{1-\nu}{2}$

Elements of the 1st type

$$\frac{E}{2(1-\nu^2)}\begin{bmatrix} \xi d & 0 & -\xi d & -d & 0 & d \\ 0 & \xi & -\nu & -\xi & \nu & 0 \\ -\xi d & -\nu & 1/\xi+\xi d & \nu+d & -1/\xi & -d \end{bmatrix}$$

Elements of the 2nd type

$$\frac{E}{2(1-\nu^2)}\begin{bmatrix} -d & -\xi & \nu+d & \xi+d/\xi & -\nu & -d/\xi \\ 0 & \nu & -1/\xi & -\nu & 1/\xi & 0 \\ d & 0 & -d & -d/\xi & 0 & d/\xi \end{bmatrix}$$

Elements of the 3rd type

$$\frac{E}{2(1-\nu^2)}\begin{bmatrix} 1/\xi+\xi d & -\nu-d & -\xi d & \nu & -1/\xi & d \\ -\nu-d & \xi+d/\xi & d & -\xi & \nu & -d/\xi \\ -\xi d & d & \xi d & 0 & 0 & -d \end{bmatrix}$$

Elements of the 4th type

$$\frac{E}{2(1-\nu^2)}\begin{bmatrix} \nu & -\xi & 0 & \xi & -\nu & 0 \\ -1/\xi & \nu & 0 & -\nu & 1/\xi & 0 \\ d & -d/\xi & -d & 0 & 0 & d/\xi \end{bmatrix}.$$

The matrix K_f of the system (7) is composed of the stiffness matrices of the elements K^e in the following way. Suppose there are l -elements (Figure 3.1), we number all the vertices from left to right and from top to bottom. The matrix K_f has a dimension of $2\cdot l\times 2\cdot l$. Let's imagine it consisting of blocks (2x2). The dimension of such a matrix will be $l\times l$. Matrices of elements, as block ones, consisting of 2x2 submatrices, have a dimension of 3x3. Let the vertices of the elements belonging to the upper layer have numbers i and (or) $i+1$, and the vertices of the elements belonging to the lower layer have numbers j and (or) $j+1$. Then the following contribution to K_f will be made:

elements of the 1st type

$$K_f(j,j)=K_f(j,j)+KL(1,1)$$

($KL(1,1)$ - are the corresponding submatrices (2x2) of the matrix $K^{(1)}$)

$$K_f(i,i)=K_f(i,i)+KL(2,2)$$
$$K_f(i+1,i+1)=K_f(i+1,i+1)+KL(3,3)$$
$$K_f(j,i)=K_f(j,i)+KL(1,2)$$
$$K_f(j,i+1)=K_f(j,i+1)+KL(1,3)$$
$$K_f(i+1,i)=K_f(i+1,i)+KL(3,2)$$

elements of the 2nd type

$$K_f(i+1,i+1)=K_f(i+1,i+1)+KL(1,1)$$
$$K_f(j+1,j+1)=K_f(j+1,j+1)+KL(2,2)$$
$$K_f(j,j)=K_f(j,j)+KL(3,3)$$
$$K_f(j+1,i+1)=K_f(j+1,i+1)+KL(2,1)$$
$$K_f(j+1,j)=K_f(j+1,j)+KL(2,3)$$
$$K_f(j,i+1)=K_f(j,i+1)+KL(3,1)$$

620

elements of the 3rd type

$$K_f(j,j)=K_f(j,j)+KL(1,1)$$
$$K_f(i,i)=K_f(i,i)+KL(2,2)$$
$$K_f(j+1,j+1)=K_f(j+1,j+1)+KL(3,3)$$
$$K_f(j,i)=K_f(j,i)+KL(1,2)$$
$$K_f(j+1,j)=K_f(j+1,j)+KL(3,1)$$
$$K_f(j+1,i)=K_f(j+1,i)+KL(3,2)$$

elements of the 4th type

$$K_f(i+1,i+1)=K_f(i+1,i+1)+KL(1,1)$$
$$K_f(j+1,j+1)=K_f(j+1,j+1)+KL(2,2)$$
$$K_f(i,i)=K_f(i,i)+KL(3,3)$$
$$K_f(i+1,i)=K_f(i+1,i)+KL(1,3)$$
$$K_f(j+1,i+1)=K_f(j+1,i+1)+KL(2,1)$$
$$K_f(j+1,i)=K_f(j+1,i)+KL(2,3)$$

625 .

It is known from finite element theory [1] that the matrix K_f is symmetric and positive definite. Therefore, the filling of elements lying only on the main diagonal and below is shown. Next, we destroy the rows and columns of the matrix corresponding to the nodes (vertices) lying on the border of
630 the selected area (except for the zero horizontal).

In the case of modeling the impact of a load on a soil layer lying on a very weak foundation (eg swamp), we do not impose restrictions on the lower boundary.

The contribution to the global load vector F_f - the right-hand side of system (7) is determined from each element by formula (8). In this case, the node with the number t corresponds to the $(2t-1)$
635 and $2t$ lines of the vector F_f . Lines corresponding to border nodes are destroyed.

After finding the nodal displacements, the value of the stresses that are constant on the element is determined by the formula (3). The values of the stresses at the nodes are found by averaging over neighboring elements.

Stress matrix σ

$$\sigma=\begin{bmatrix}\sigma_x\\ \sigma_z\\ \tau_{xy}\end{bmatrix} .$$

Let's introduce the notation:

$$K_\sigma=\frac{E}{(1-\nu^2)h_1h_2} \quad ; \quad \alpha=\frac{1-\nu}{2} \quad ;$$

$$u_{12}=u_1-u_2,\ u_{13}=u_1-u_3,\ u_{23}=u_2-u_3,$$
$$v_{12}=v_1-v_2,\ v_{13}=v_1-v_3,\ v_{23}=v_2-v_3 .$$

Elements of the 1st type

$$\sigma=K_\sigma\begin{bmatrix}-h_2u_{23}+\nu h_1v_{12}\\ -\nu h_2u_{23}+h_1v_{12}\\ \alpha[h_1u_{12}-h_2v_{23}]\end{bmatrix}$$

Elements of the 2nd type

$$\sigma=K_\sigma\begin{bmatrix}h_2u_{23}-\nu h_1v_{12}\\ \nu h_2u_{23}-h_1v_{12}\\ -\alpha[h_1u_{12}+h_2v_{23}]\end{bmatrix}$$

Elements of the 3rd type

$$\sigma=K_\sigma\begin{bmatrix}-h_2u_{13}+\nu h_1v_{12}\\ -\nu h_2u_{13}+h_1v_{12}\\ \alpha[h_1u_{12}-h_2v_{13}]\end{bmatrix}$$

Elements of the 4th type

$$\sigma=K_\sigma\begin{bmatrix}h_2u_{13}-\nu h_1v_{12}\\ \nu h_2u_{13}-h_1v_{12}\\ -\alpha[h_1u_{12}+h_2v_{13}]\end{bmatrix} .$$

Further, according to the formulas of section (2), we determine the initial values of pressures, heads

and stresses.

4. Calculation results

The figures below show the results of calculating the zones of vertical stresses from the impact of the ML-56 machine for different types of tires:

33L-32F134;

33L-32F134M - with reduced pressure;

71x47-25; 79x59-26} ultra wide-profile.

Movement on loamy soil is simulated. The soil is presented in two layers: a thin layer of 30 cm on a denser base. The relative humidity of the soil is 80%. The characteristics of the soil are presented in the table.

	Deformation modulus $E,\ kg/cm^2$	Poisson's ratio ν	Internal grip $C_o,\ kg/cm^2$	Internal friction angle $\varphi_o,\ grad.$
Upper layer	100	0,3	0,21	15
Bottom layer	370	0,3	0,60	18

Soil characteristics

An intensive increase in rutting can be expected during trips by the machine with 33L-32F134 tires as a result of vertical deformation in the soil and lateral uplift caused by the movement of destroyed soil into zones with zero and negative (i.e. tensile) vertical stresses. This is the manifestation of the flat phenomena of the mathematical model.

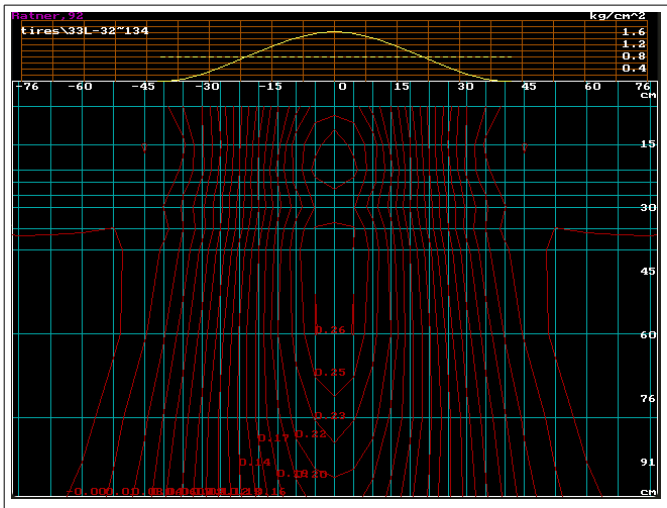

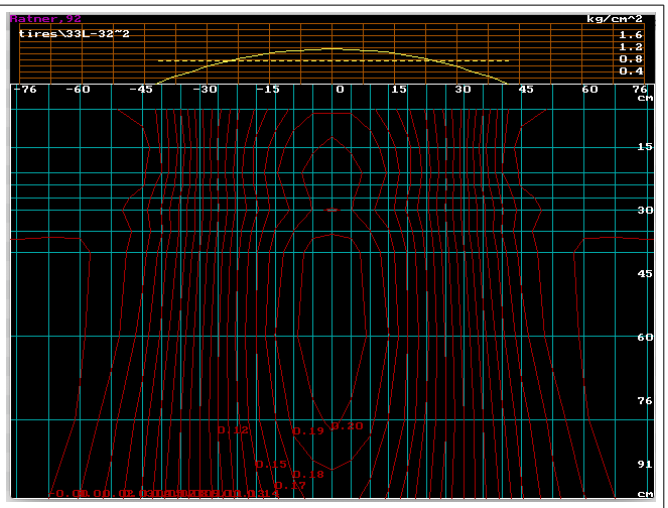

Comparing the figures, we can note the absence of soil zones with a destroyed structure (figure on the right) in the case of using the 33L-32F134M tire with an internal air pressure of 0.8 kg / cm ^ 2. This is due to a change in the shape of the loading diagram with a decrease in the internal air pressure from

1.4 to 0.8 kg / cm ^ 2.

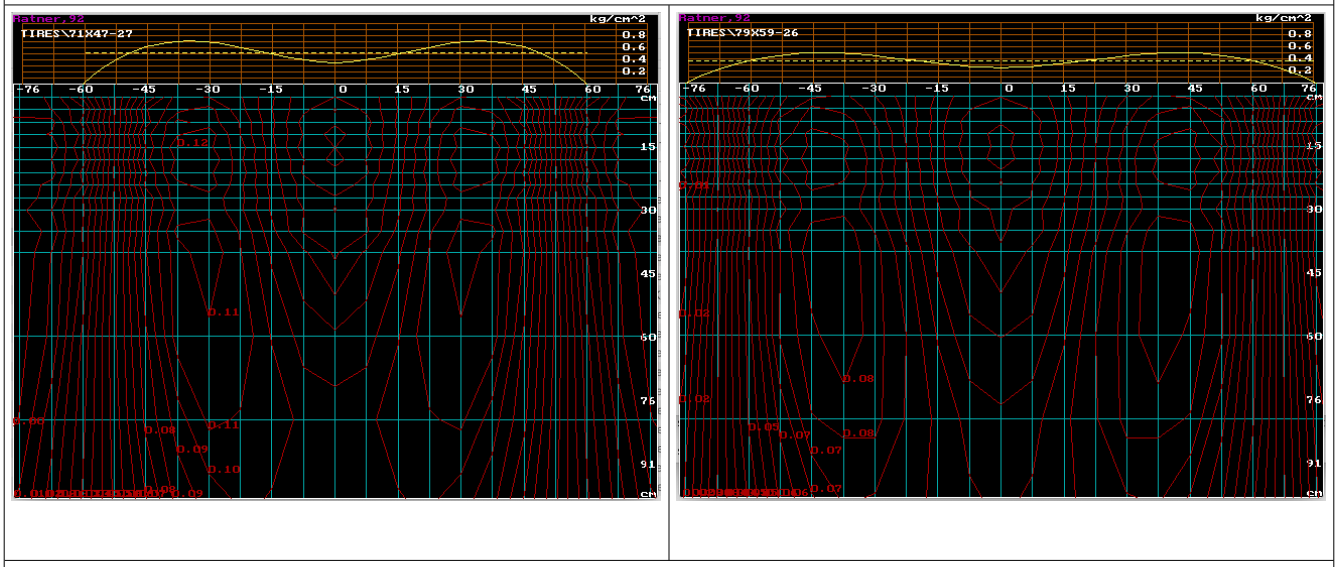

A significant reduction in the stress state of the soil is observed with the use of ultra-wide-profile tires.

675

5. Experimental data

The following figures show the calculated zones of vertical stresses from the impact of the TT-4M tractor with a highly elastic and serial track. The soil is homogeneous (in modulus of deformation), therefore, an analytical solution to the first boundary value problem is presented. The characteristics of
680 the soil are presented in table 3.1. Available experimental data (mean values of pressure sensors over time series) are presented in Table 3.2. These data were obtained by a group of employees of the laboratory of basic forestry tractors of the Central Research Institute of Mechanization And Energy Of The Forest Industry: L.M. Emaikin, M.O. Sokolov, L.N. Trubachev and S.N. Krapukhin. The tests were carried out in the fall of 1992 in accordance with the subject of work on the creation of a highly
685 elastic propulsive device. The head of the group is a senior researcher, Candidate of Technical Sciences A.P. Kuznetsov.

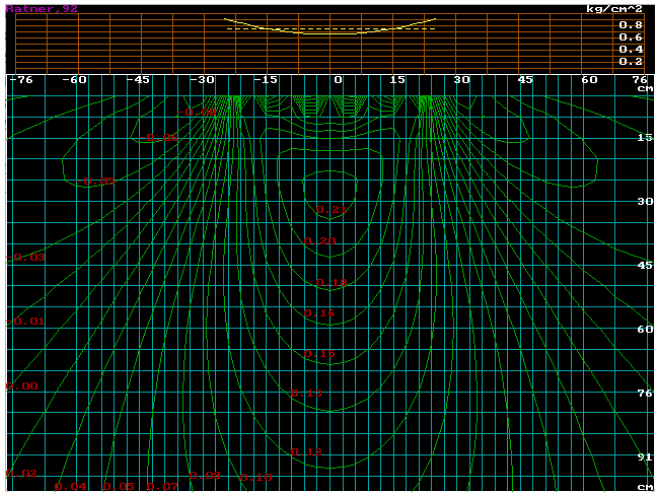

Distribution of initial stresses σ_{zo}, kg/cm^2 *in a homogeneous medium. Serial track.*

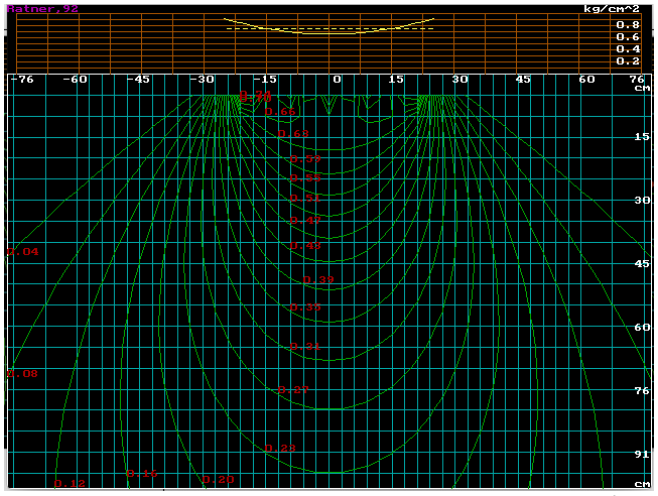

Distribution of steady-state stresse σ_z, kg/cm^2 *in a homogeneous medium. Serial track.*

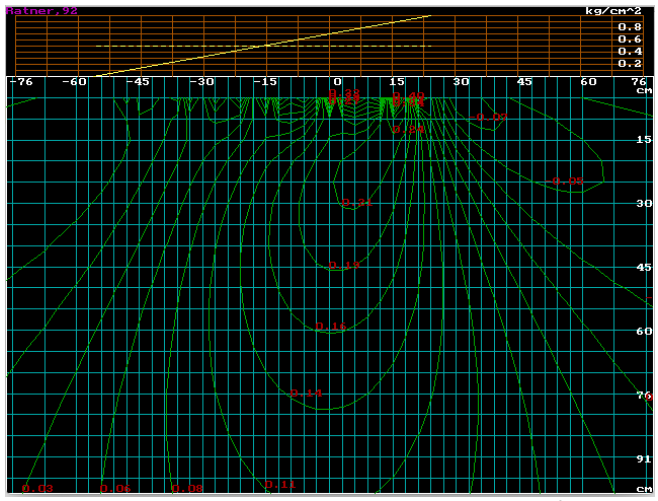

Distribution of initial stresses σ_{zo}, kg/cm^2 *in a homogeneous medium. Highly elastic track.*

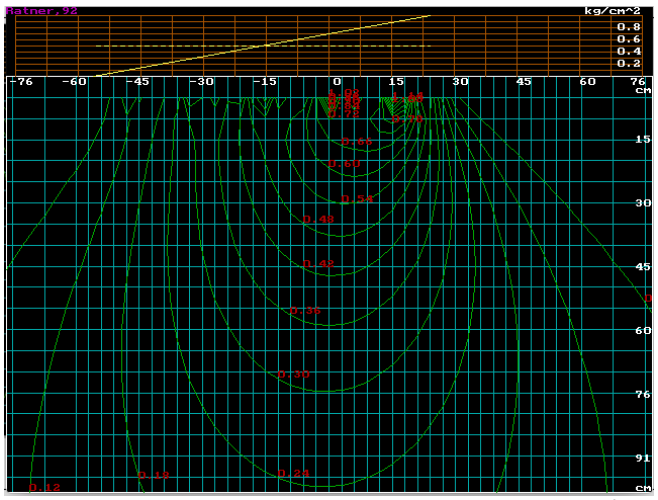

Distribution of steady-state stresse σ_z, kg/cm^2 *in a homogeneous medium. Highly elastic track.*

Sampling depth, cm	The number of strikes by the Soyuzdorniya striker	Soil deformation modulus for Soyuzdorniya striker, MPA	Density of wet soil g/cm^3	Density of the soil skeleton g/cm^3
20	3.33	5.0	2.04	1.7
40	4.0	6.0	2.02	1.68
60	2.75	4.12	2.11	1.74

Table 3.1 Physical and mechanical indicators of soils and grounds on measured plots

Distance from the center of the treadmill to the pressure sensors, cm			
	-25	0	25
Serial track. Gross weight of the tractor 21250 kg			
Top row	0.090	0.384	...
+ 20 см	0.196	0.333	0.357
+ 40 см	...	0.231	...
Highly elastic track. Gross weight of the tractor 23900 kg			
Top row	0.060	...	1.538
+ 20 см	0.190	0.282	0.289
+ 40 см	...	0.189	...

Table 3.2 Average values of pressures, kg/cm^2

It can be seen from Table 3.2 that the general view of the calculated distribution functions of vertical stresses for both types of tracks is in good agreement with the experimental data. The experimental values of stresses are greater than the initial calculated values, but less than the steady-state values of stresses. This can be explained by the following factors:

a) the initial distance from the top layer of the sensors (20 cm) decreased as a result of soil deformation;

b) the values of pressures averaged over the time series are taken as experimental data, i.e. pressure from the load, which acts for some time, and the initial stresses from the instantly applied load are taken as the calculated ones, the value of which is averaged over the reference area of the track;

c) pressure sensors perceive the load, the components of which are the load from water pressure and the load from vertical stresses in the soil skeleton, and we calculate only vertical stresses in the skeleton.

Conclusion

The presented mathematical model, together with its software implementation, makes it possible to assess the degree of influence of the tire of a forest wheeled tractor on the waterlogged forest soil, depending on the design parameters of the tire and the vertical loads that fall on it.

The adequacy of the mathematical model is confirmed by the conducted experimental studies, as well as by numerous test results of forest wheeled tractors.

The model is developed based on the theory of soil mechanics. The plane problem of compaction of water-saturated anisotropic (in the general case) soil is considered. It was shown that with an instantaneous application of a vertical load, the initial distribution of stress and water pressure in the soil are expressed through their values in a state of complete stabilization. Therefore, it is

conventionally assumed that the magnitude of the load does not change before the onset of this state, causing linear (relative to the load) deformations of the soil.

Thus, first, a plane problem of different modulus of the theory of a linearly deformable medium is solved. This problem is described by a system of partial differential equations (equations (7-9) of section 1). The solution is found by the finite element method with respect to displacements. Then, the steady-state and initial values of the stresses are determined, as well as the values of the maximum deviation of the total stress vector - θ_{max} .

In the case of an isotropic medium, the initial heads function (H_o) satisfies the Laplace equation: $\Delta H_o = 0$. The first boundary value problem is posed and solved. Analytical expressions are obtained for the initial values of water heads, pressure and stresses. With their help, one can select the optimal triangulation of the region for a given loading diagram and check the finite element solution.

The initial data for this mathematical model are the layer-by-layer values of the deformation modulus, Poisson's ratio, adhesion coefficient C_o , and angle of internal friction φ_o . Condition: $\theta_{max} = \infty$ means that the soil mass is in a state of ultimate plastic equilibrium.

The calculation results are presented as level lines of the function of two variables. The general view of the vertical stress function is in good agreement with the available experimental data.

It was found that the form of the transverse loading diagram has a significant effect on the degree of the stress state of the soil. At the same average contact pressures, the parabolic shape of the loading diagram, which is characteristic of tires with reduced internal air pressure, has the smallest effect on the soil.

The method can serve as the basis for predicting the degree of soil compaction and the intensity of rutting, as well as the environmental consequences of the operation of forest machines.

Computer Code Availability

Name of code: soil models;

developer: Dr. Igor Ratnere, Lawrence Berkeley National Laboratory
1 Cyclotron Road, M/S 91R0183, Berkeley, CA 94720, 510-495-8373 (Office), iratnere@lbl.gov

year first available: 1992

hardware required: Mac (Mac OS) or PC (Windows)

software required: DosBox, Turbo Pascal

https://gist.github.com/nvgrw/da00b5d3ac96b9c45c80

program language: Turbo Pascal

program size: 400 K

https://iratnere@bitbucket.org/iratnere/soil-models.git

Main software modules:

MKESol - control module;

UnCode - contains subroutines for identifying the area of the partition;

SplinUnt - contains subroutines for constructing an interpolation cubic spline and for outputting spline

values at specified points;

GetSpline - the procedure for forming the global load vector (the right side of the linear algebraic system of equations);

GetData - procedure for generating a global stiffness matrix;

LDL - contains routines for decomposition and solutions for strip matrices by the Cholesky method [7].

After the MKESol program has been processed, the values of the grid functions from the space V that define the vertical and horizontal displacements are known. These values are recorded in the Output.mke file;

MKEDrow - control module for presenting calculation results;

Sigma - contains programs for calculating mesh functions from a subspace $U_{1,}\ldots, U_s$. The initial data is the values of the mesh displacement functions contained in the Output.mke file;

FuncLoad - contains numerical integration routines for finding a solution to the first boundary value problem in the case of an isotropic medium;

Anal - contains subroutines for graphical representation of a grid function in the form of function level lines of two variables. This representation is performed by the LineLab (Nf, k) procedure. Here Nf is a parameter defining the identifier code of the grid function; k is the number of level lines on the display screen.

Nf	Level line
0	σ_x - steady-state stresses along the axis x, kg/cm^2
1	σ_z - steady-state stresses along the axis z, kg/cm^2
2	τ_{xz} - steady-state shear stresses along the axis x, kg/cm^2
3	σ_{xo} - initial stresses along the axis x, kg/cm^2
4	σ_{zo} - initial stresses along the axis z, kg/cm^2
5	P_o - initial pressures, kg/cm^2
6	V - vertical deformations, cm
7	Θ_{max} - the maximum angle of deviation of the full stress vector, $grad$
Encoding for solving the First Boundary Value Problem (FuncLoad module)	
10	σ_{xo} - initial stresses along the axis x, kg/cm^2
11	σ_{zo} - initial stresses along the axis z, kg/cm^2
12	P_o - initial pressures, kg/cm^2

Nf encoding table

References

1. Ciarlet P.G. 1980. The finite element method for elliptic problems. Mir, M., 512 pp. [in Russian]

2. Gersevanov N.M., 1948. Research in the field of soil dynamics, mechanics and applied mathematics. Stroyvoenmorizdat, M., 376 pp. [in Russian]

3. Florin, V.A.,1954. Fundamentals of Soil Mechanics, Vol.1. Gosstroyizdat, M., 358 pp. [in Russian]

4. Florin, V.A.,1961. Fundamentals of Soil Mechanics, Vol.2. Gosstroyizdat, M., 544 pp. [in Russian]

5. Nikiforov A.F. 1983. Methods of Mathematical Physics. Ed. Moscow State University, M., 224 pp. [in Russian]

6. Pokrovsky, G.I. 1941. Friction and traction in soils. Stroyizdat, M., 120 pp. [in Russian]

7. Rainsch Wilkinson. 1976. Algorithms reference book in the Algol language. Linear algebra. Mechanical engineering, M., 392 pp. [in Russian]

8. Ratner I.S. 1993. Determination of traction reference indicators of a wheeled forestry tractor and assessment of soil condition parameters. Dissertation for the degree of candidate of technical sciences. Khimki, 215 pp.
9. Terzagi K. 1961. Theory of soil mechanics, Stroyizdat, M., 508 pp. [in Russian]
10. Timoshenko SP, Gyd'er J. 1975. Theory of elasticity. Science, M., 576 pp. [in Russian]